Adsorption (2014) 20:341–348
DOI 10.1007/s10450-013-9597-1

The adsorption properties of organic sulfur compounds on zeolite-based sorbents impregnated with rare-earth metals

Suk Yong Jung · Jung Mo Moon · Soo Chool Lee · Sang Cheol Paik · Ki Soo Park · Jae Chang Kim

Received: 15 May 2013 / Accepted: 27 November 2013 / Published online: 5 December 2013

Abstract Dimethyl disulfide (DMDS) and dimethyl sulfide (DMS) are non-polar, stable, organic sulfur compounds found in liquefied petroleum gas, and their oxidation in the atmosphere results in the formation of tropospheric sulfur dioxide, which is subsequently converted into sulfuric acid, as the main factor of acid rain. In the present study, adsorption processes were devised based on the use of modified zeolite impregnated with rare-earth metals (Ce, La or Pr) for the adsorption of DMDS and DMS, and their sorption capacities were compared with that of commercial zeolite [Zeolite-Y, Ultra Stable Y(USY)]. The adsorption capacities of adsorbents were tested using a micro liquid flow reactor at room temperature. USY impregnated with cerium oxide (UC-10) had excellent DMDS and DMS adsorption capacities as compared with the other adsorbents tested. It was found that impregnation of USY with rare-earth metal such as Ce improved the sulfur adsorption capacity of zeolite. The form of the Ce promoter impregnated into USY was determined by FT-Raman spectroscopy. Adsorbents were characterized by X-ray fluorescence spectrometer, X-ray diffraction, and BET and the results obtained are discussed.

Keywords Adsorbent · Adsorption · Organic sulfur compounds · DMDS · DMS

1 Introduction

Dimethyldisulfide (DMDS) and dimethylsulfide (DMS) are non-polar, stable, organic sulfur compounds which are present in liquefied petroleum gas (LPG) (Andersen et al. 2012). During the LPG production process, DMDS and DMS compounds are produced from organic sulfur compounds like methylmercaptan (MM) and ethylmercaptan (EM), which are more toxic and have stronger smells than DMDS or DMS compounds. However, sulfur compounds like DMDS and DMS must be removed, because both are converted into SO_x when LPG is combusted, and SOx is a known precursor of acid rain, and its emission into the atmosphere is controlled and monitored based on regulations of many governments, including those of the EU and USA, as well as Korea. Furthermore, environmental regulations regarding the release of sulfur compounds to the atmosphere have been gradually strengthened (Bentley and Chasteen 2004), and thus, sulfur removal is an important step during LPG manufacture and is achieved using the merox process. During this process, sulfur concentrations are reduced by converting MM and EM to DMDS or DMS, respectively. However, using this process it is not possible to reduce the levels of sulfur compounds like DMDS and DMS to below 1 ppm (Basu et al. 1993). In addition, the alternative process, catalytic hydrodesulfurization (HDS) is the conventional method, though it is a highly inconvenient and very expensive process (Gochi et al. 2005). To

Suk Yong Jung and Jung Mo Moon have contributed equally to this study.

S. Y. Jung · S. C. Lee
Research Institute of Advanced Energy Technology, Kyungpook National University, Taegu 702-701, Korea

J. M. Moon · J. C. Kim (✉)
Department of Chemical Engineering, Kyungpook National University, Taegu 702-701, Korea
e-mail: kjchang@knu.ac.kr

S. C. Paik · K. S. Park
S-Oil Corporation, Sanam-ri, Onsan-eup, Ulju-gun, Ulsan 689-892, Korea

decrease sulfur compound levels to less than 1 ppm, adsorption processes (based on the use of adsorbents like activated carbon, zeolite, and metal oxides), absorption (Eric et al. 2012), catalytic oxidation (Devulapelli and Demessie 2008; Demessie and Devulapelli 2009), plasma destruction (Chen et al. 2012, Jarrige and Vervisch 2007), and photo catalytic oxidation (Chen and Jang 2012, Demeestere et al. 2005; He et al. 2009, Jo and Hwang 2011) processes have been devised. However, these processes, with the exception of adsorption, consume much energy (Hwang and Tai 2010), and thus adsorption processes have attracted considerable attention. Various adsorbents have been applied to the manufacture of liquid natural gas (LNG), gasoline, diesel, and wastewater treatment processes. In particular, adsorbents have been devised to remove organic sulfur compounds like mercaptan-base, thiophene-base, and methyl sulfide-base compounds in LNG. Cui and Turn (2009) and Hwang and Tai (2011) reported on the DMS adsorption properties of modified activated carbon impregnated with iron chlorides and of ion-exchanged zeolites. Bashkova et al. (2002) and Kim and Yie (2005) reported that modified activated carbon with a micro-pore size and activated carbon impregnated with copper chloride exhibited improved adsorption capacities for organic sulfur compounds, such as MM and DMDS. Caleron et al. (2012) reported the adsorption properties of an iron nano-particle adsorbent in a batch reactor with respect to the removal of DMDS. Park et al. (2010) investigated the removals of organic sulfur compounds, such as, the MM, EM, DMDS, and DMS, from C4 oil using modified zeolites impregnated with alkali-metal carbonates (Park et al. 2011). The sulfur adsorbing capacities of these adsorbents ranged from 2.5 to 4.0 mg S/g sorbent, but they were not investigated with respect to regeneration or long-term stability. Rare earth metal oxide based adsorbents, like CeO_2 based adsorbents, have been studied with respect to the selective removal of organic sulfur compounds from gasoline, diesel, and jet fuel (Watanabe et al. 2003, 2004). Furthermore, CeO_2 is known to be an excellent support and promoter for the removal of SOx from flue gas and natural gas. Watanabe reported on the sulfur adsorption properties of CeO_2-based adsorbents with respect to the removal of organic sulfur compounds from gasoline. It was found that the sulfur adsorption capacities of La-CeO_2 and Y-CeO_2 adsorbents were very high at about 8.5 mgS/g sorbent, but that their regeneration properties and long-term stabilities were not examined (Watanabe et al. 2004). Thus, despite numerous efforts to develop adsorbents capable of removing organic sulfur compounds from fossil fuels, all adsorbents described in the literature have some limitations, such as, low sulfur adsorption capacity, unknown regeneration properties, or dubious long-term stability. Furthermore, the effects of real LPG on adsorbent characteristics have not yet been evaluated. In the present study, to improve the ability to adsorb sulfur-containing compounds, we produced adsorbents by impregnating with rare-earth metals Ce, La, and Pr and investigated their performances in a liquid flow reactor. In addition, we examined their regenerative abilities and long-term stabilities, as their abilities to process real LPG.

2 Experiment

2.1 Preparation of adsorbents

In this work, the various modified adsorbents were prepared to remove sulfur compounds from LPG and were tested using a fixed liquid flow reactor. The modified adsorbents, that is, USY-based adsorbents promoted with the rare-earth metals Ce (cerium), La (lanthanum) and Pr (promethium) were prepared by an impregnation method. These adsorbents are named UC-10, UL-10, and UP-10, respectively. The amount of rare-earth metal used was calculated to 10 wt% of the adsorbent. The precursors used were cerium nitrate [$Ce(NO_3)_3$], lanthanum nitrate [$La(NO_3)_3$] and promethium nitrate [$Pr(NO_3)_3$], each of which was dissolved in water. USY commercial adsorbent was added to the rare-earth metal solutions, each of which were stirred for 12 h at room temperature, evaporated to dryness using evaporator, and then heat treated at 150 °C for 4 h followed by 400 °C for 12 h. Commercial adsorbents, namely, zeolite Y and USY (Ultra-Stable Y) were used to compare the sulfur adsorption capacities of the prepared adsorbents. Information of the commercial zeolite Y and USY adsorbents are summarized in Table 1. Zeolite Y and USY were purchased from Sigma Aldrich and UOP, respectively. The cation type of both commercial adsorbents is Na^+ form, and the Si/Al ratios are 1.5(Zeolite Y) and 2.9(USY), respectively, as determined by X-ray fluorescence spectrometer (XRF) analysis. The particle sizes of both commercial adsorbents were below 3 μm.

Table 1 Information of the commercial Zeolite Y and USY adsorbent

Commercial sample name	Company	Si/Al ratio	Type of cation	Particle size (μm)
Zeolite Y	Sigma Aldrich	1.5	Na^+	<3
USY	UOP	3.0	Na^+	<3

The Si/Al ratio was measured by XRF analysis

Table 2 Experimental conditions

	Adsorption process	Regeneration process
Adsorbent amount (g)	0.5	0.5
Temperature (°C)	30	280
Flow rate (mL/min)	6.0	100
Pressure (bar)	1–10	1
Composition	DMDS 20 PPMW DMS 20 PPMW *n*-Hexane balance	N_2

2.2 Standard solution preparation and experimental conditions

To evaluate the sulfur adsorbing capacities of the adsorbents, we used a standard solution, which was prepared by adding DMDS (Aldrich, 99 %) and DMS(Aldrich, 99 %) at 100 PPMW to 1 l of *n*-hexane (Merck, 98 %), and then gradually diluted this solution with *n*-hexane to DMDS and DMS concentrations of 20 PPMW. Table 1 summarizes the experimental conditions used. As shown in Table 1, under atmospheric conditions using the standard solution, 0.5 g of adsorbent was packed into the reactor, which was operated at a feed flow rate and temperature of 6 mL/min and 30 °C. Under high pressure conditions using real LPG, the pressure was increased to 10 bars, though the feed flow rate and the temperature were not changed. For the regeneration process, the regeneration gas was N_2, which was applied at a flow rate of 100 mL/min, and the temperature was gradually increased from room temperature to 280 °C for 30 min, and then maintained for 4 h. We refer to this desulfurization/regeneration process as 1 cycle (Table 2).

2.3 Apparatus

To determine the sulfur adsorption capacities of sorbents using various pressures, stainless steel was used for the reactor and line of the fixed bed reactor system. Adsorbents were packed in a stainless steel reactor of internal diameter 1.27 cm and length 6 cm. The standard solution or LPG was fed to the reactor using a HPLC pump. Reaction and regeneration temperatures were controlled using an electric furnace. The N_2 regeneration gas was fed into the reactor and controlled using a mass flow controller (MFC). During regeneration, the line temperature was increased to 80 °C to prevent the condensation and re-adsorption of sulfur compounds. A HP 6890 gas chromatography equipped with a flame photometric detector (FPD), and a Supel-Q (Plot) (30 m × 0.53 mm) column at inlet, oven, and detector temperatures of 210, 200 and 230 °C, respectively, were used to determine the sulfur adsorption capacities of the sorbents and GC runs were performed every 5 min.

2.4 Characterizations of various adsorbents

Textural properties such as surface area, pore volume and average pore size were obtained by nitrogen adsorption at liquid N_2 temperature using ASAP2020 (micromeritics). The micro- and meso-pore volumes were calculated by the T-plot. In addition, the micro- and meso-pore sizes were calculated from the adsorption isotherm using the density functional theory (DFT) method and Barrett, Joyner, Halenda (BJH) desorption method. The components and amount of the adsorbents were analyzed by the FP method using a Rh X-ray tube in a Philips PW2400 X-ray fluorescence spectrometer (XRF). The crystal structures of the adsorbents were analyzed using a Cu Kα radiation source in a Phillips XPERT X-ray diffraction (XRD) unit analysis at the Korea Basic Science Institute in Daegu. In addition, to investigate the form of the cerium component by the FT-Raman analysis, spectrum GX and Autoimage of Perkin-Elmer was used. The Beam splitter (Ge coated on KBr) and DTGS detector kits allow the range 7,000–50 cm^{-1} to be covered with a maximum resolution of 0.3 cm^{-1}.

3 Results

3.1 Sulfur adsorption performance of various adsorbents

Breakthrough curves are thought to provide the best means of determining sorbent adsorption capacities of sulfur compounds. In a typical fixed-bed experiment, DMDS and DMS concentrations below 1 ppm in the outlet solution from the reactor were negligible. Breakthrough time was defined as the time required for the DMDS or DMS concentration in the outlet solution to reach 1 ppm. Figure 1 shows the DMDS breakthrough curves (a) and DMDS adsorption capacities (b) for the first cycle for Zeolite Y, USY, UC-10, UL-10, and UP-10 adsorbents, for an inlet DMDS concentration (C_0) of 20 ppm in hexane at 30 °C. The feed flow rate and liquid hourly space velocity (LHSV) were 6 mL/min and 360 h^{-1}, respectively. As shown in Fig. 1a, The X-axis and Y-axis show the reaction time and the concentration of DMDS emitted from the reactor, respectively. The DMDS breakthrough times of the commercial adsorbents Zeolite Y and USY were 6 and 9 min, respectively, after which the DMDS concentration rose rapidly up to the inlet DMDS concentration. In addition, in the case of modified adsorbents such as UC-10, UL-10 and UP-10 adsorbents, their DMDS breakthrough times were 72, 15, and 18 min, respectively, and the DMDS

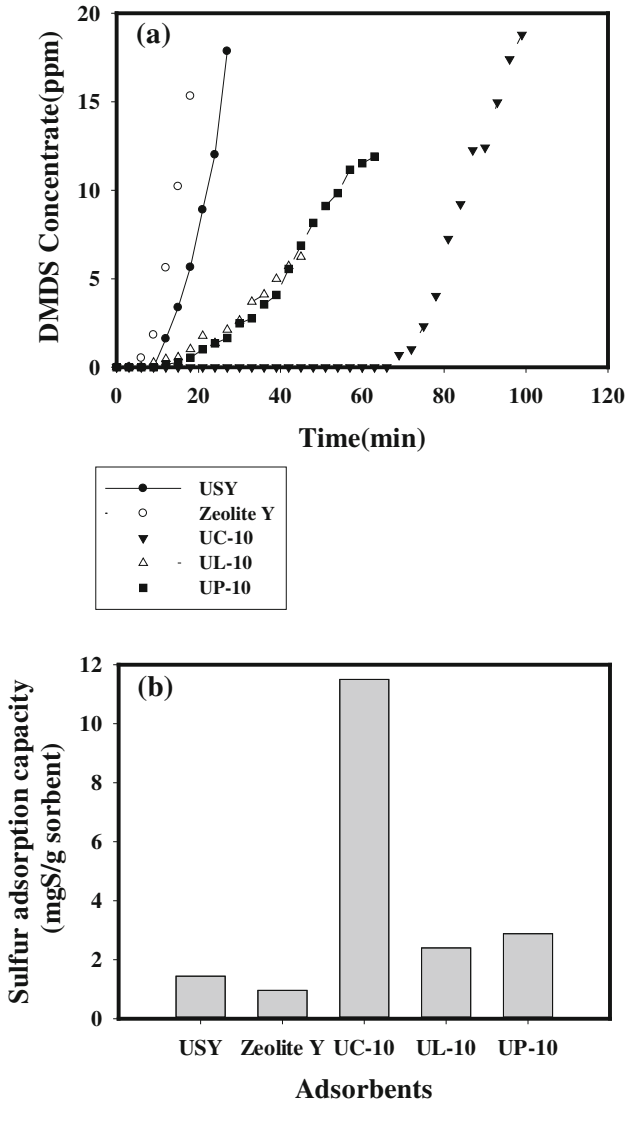

Fig. 1 Breakthrough curves **a** and sulfur adsorption capacities **b** of various adsorbents for DMDS

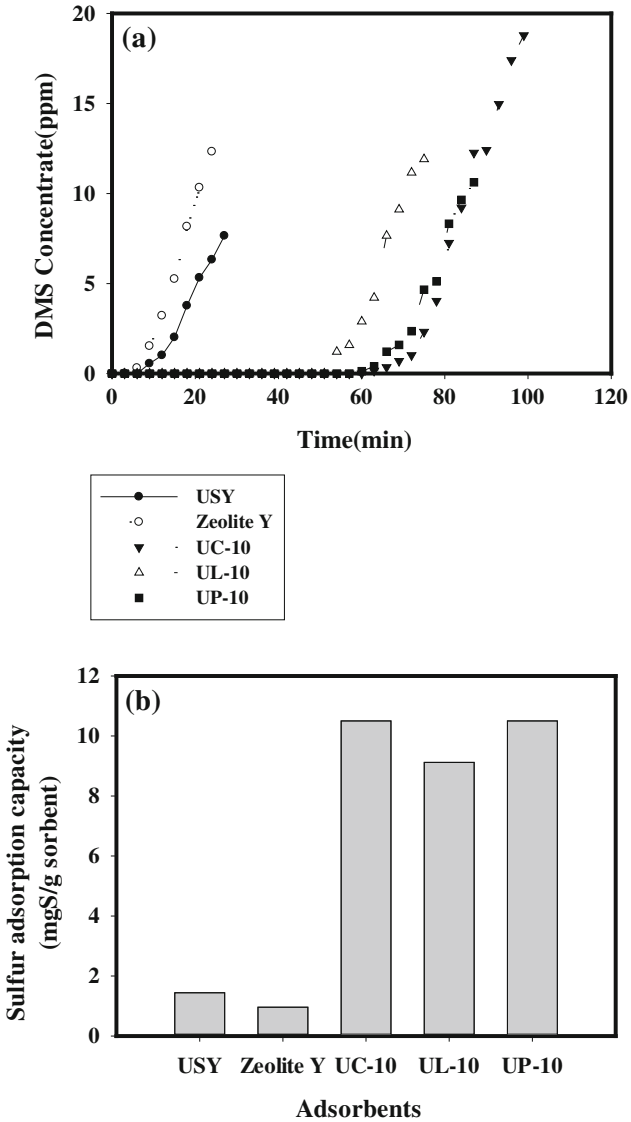

Fig. 2 Breakthrough curves **a** and sulfur adsorption capacities **b** of various adsorbents for DMS

concentration rose gradually up to the inlet DMDS concentration. The DMDS adsorption breakthrough time of UC-10 adsorbent was greater than those of UL-10 or UP-10 adsorbents. Figure 1b summarizes the sulfur adsorption capacities of the different adsorbents. The vertical axis indicates the amount of sulfur absorbed per 1 g of sorbent before the DMDS concentration in the outlet solution reached 1 PPMW. As shown in Fig. 1b, DMDS adsorption capacities of Zeolite Y, USY, UC-10, UL-10 and UP-10 adsorbents were 1.44, 0.96, 11.5, 2.4 and 2.88 mgS/g sorbent, respectively. It was found that the DMDS adsorption capacity of UC-10 adsorbent was higher than those of the other adsorbents. Figure 2 shows the DMS breakthrough curves (a) and DMS adsorption capacities (b) for first cycles of the adsorbents Zeolite Y, USY, UC-10, UL-10 and UP-10 adsorbents, where the inlet DMS concentration was 20 ppm in hexane at 30 °C. As shown in Fig. 2a, the DMS breakthrough times of Zeolite Y, USY, UC-10, UL-10 and UP-10 adsorbents were 6, 9, 66, 57 and 66, respectively, after which the DMS concentration rose rapidly to the inlet DMS concentration. In addition, as shown in Fig. 2b, the DMS adsorption capacities of the Zeolite Y, USY, UC-10, UL-10 and UP-10 adsorbents were 0.96, 1.44, 10.5, 9.12 and 10.5 mgS/g sorbent, respectively. It was found that the DMS adsorption capacity of the UC-10 adsorbent was also higher than those of the other adsorbents. Overall, the DMS and DMDS adsorption performances of Zeolite Y and USY were 1.5–1 mgS/g sorbent. For UP-10 and UL-10 sorbents, DMS adsorption capacities were relatively high, but DMDS adsorption capacities were not, that is, La and Pr promoters more

selectively adsorbed DMS than DMDS. However, UC-10 adsorbent had higher adsorption capacities for DMDS and DMS than the other experimental adsorbents. It was found that the adsorption performance of UC-10 adsorbent for both DMDS and DMS was improved by Ce promoter.

3.2 The physical properties of various adsorbents

Surface areas and pore size distributions of the various adsorbents, consisting USY impregnated with Ce, Pr and La, were analyzed by XRF and nitrogen adsorption, to investigate the change of physical properties. First, to investigate the impregnated amounts of Ce, Pr and La in UC-10, UP-10 and UL-10 adsorbents, they were analyzed by the semi-quantity of XRF, the results of which are summarized in Table 3. As shown in Table 3, USY was found to be comprised of, Na, Al, Si and O, as 1.8, 12.0, 34.9 and 51.3 wt%, respectively. The Si/Al ratio of USY was about 2.91, and as mentioned previously, the cation of USY was sodium ion. In the case of UC-10, UP-10 and UL-10 adsorbents, the amount of rare earth metals Ce, Pr and La in each adsorbent was approximately 10 wt%. It was found that the impregnated amount of the rare earth metals was well reflected the calculated amount. The Si/Al ratios of UC-10, UP-10 and UL-10 adsorbents ranged from 3.2 to 3.5. Although the Si/Al ratios of UC-10, UP-10 and UL-10 adsorbents were slightly increased as compare to that of the USY adsorbent, the structure of the USY like support was not broken. The physical properties (surface area, pore volume and pore size) of all adsorbents were determined by BET analysis, the results of which are summarized in Table 4. The automatic nitrogen adsorption apparatus was an ASAP2020 unit (micromeritics co.), and the micro and macro pore sizes of all adsorbent were calculated by the DFT-method and BJH Desorption pore size-method. The pore volume was calculated by t-plot method at each micro and macro pore size scale of the adsorbent. As shown in Table 4, the surface areas of USY, UC-10, UP-10 and UL-10 adsorbents were 743.9, 551.1, 440.4 and 482.6 m^2/g, respectively, and their total pore volumes were 0.3325, 0.2415, 0.2617 and 0.2594 cm^3/g, respectively. These results reveal that the surface area and pore volume of UC-10, UP-10 and UL-10 adsorbents were reduced as compared to those of the USY adsorbent. In addition, their main micropore sizes and pore volumes were approximately 0.42–0.5 nm and 0.20–0.26 cm^3/g, respectively. Their main mesopore sizes and pore volumes were approximately 5.0–5.4 nm and 0.05–0.076 cm^3/g, respectively. The adsorption capacity of an adsorbent increases in proportion to surface area and pore volume of adsorbent. Thus, our findings regarding surface areas and pore volume indicate that the adsorption capacities of UC-10 adsorbent for DMDS and DMS should be lower than that of USY, but as shown in Figs. 1 and 2, the DMDS and DMS adsorption capacities of the UC-10 adsorbent were greater. In addition, in the case of the UC-10, UP-10 and UL-10 adsorbents, their physical properties (surface area, pore size and volume) were similar, as were their DMDS and DMS adsorption capacities. However, the DMDS adsorption capacities of UP-10 and UL-10 adsorbents were lower than that of UC-10 adsorbent. So, surface area and pore volume were not found to have critical influences on sulfur adsorption capacity. In other words, the DMDS and DMS adsorption capacities of UC-10 adsorbent can be attributed to the presence of Ce, rather than to surface area or pore volume. It was found that the Ce promoter plays important role for DMDS and DMS adsorption capacities.

Table 3 Results of XRF analysis of the various rare-earth metals

Sample	Element (wt%)							Si/Al ratio
	Na	Al	Si	O	Ce	Pr	La	
USY	1.8	12.0	34.9	51.3				2.91
UC-10	0.8	9.9	31.8	47.4	10.0			3.21
UP-10	0.9	9.6	32.6	47.0		9.9		3.39
UL-10	0.6	9.3	32.3	48.0			9.8	3.47

3.3 The characterization of USY and UC-10 adsorbents

In previous results as shown in Figs. 1 and 2, the DMS adsorption capacities of UP-10 and UL-10 adsorbents were higher than DMDS adsorption capacities. The reason for the higher DMS adsorption capacity has not yet been determined. However, it was found that the total sulfur adsorption capacity of DMDS and DMS of the UP-10 and UL-10 adsorbents was lower than that of the UC-10 adsorbent. As DMDS and DMS coexist in commercial LPG, they must be simultaneously removed. Hence, the UC-10 adsorbent is best suited to the removal of organic sulfur compounds like DMDS and DMS in commercial LPG, as it has the best DMDS and DMS joint adsorption capacity. Therefore, we are focused on further analysis of the UC-10 adsorbent which was analyzed by XRD and FT-Raman to find the Ce form. Figure 3 shows the XRD patterns of the USY and UC-10 adsorbents. As shown in Fig. 3, the crystal structure of the UC-10 adsorbent was similar to that of USY, and no Ce-based crystal structure was observed. It is believed that the Ce-based crystal structure was of amorphous form in the UC-10 adsorbent. To investigate the crystal structure of Ce, UC-10 adsorbent was analyzed by FT-Raman spectroscopy. Figure 4 shows the FT-Raman results of the UC-10, USY adsorbent and commercial CeO_2. As shown in Fig. 4, no characteristic peak was observed for USY, and for CeO_2, only one peak was observed at 467 cm^{-1}, which is characteristic of CeO_2.

Table 4 Physical properties of USY and UC-10 adsorbents

Adsorbents	Total pore volume (mL/g)	Surface area (m^2/g)	Micropore		Mesopore	
			Main micropore size (nm)	Micropore volume (mL/g)	Main mesopore size (nm)	Mesopore volume (mL/g)
USY	0.3325	743.9	0.50	0.2564	4.95	0.0761
UC-10	0.2415	551.1	0.42	0.1922	5.15	0.0493
UP-10	0.2617	440.4	0.43	0.2032	4.97	0.0585
UL-10	0.2954	482.6	0.42	0.2213	5.42	0.0741
CeO_2	0.0350	9.2	–	–	9.58	0.0350
Zeolite Y	0.3232	610.8	0.38	0.3008	–	0.0224

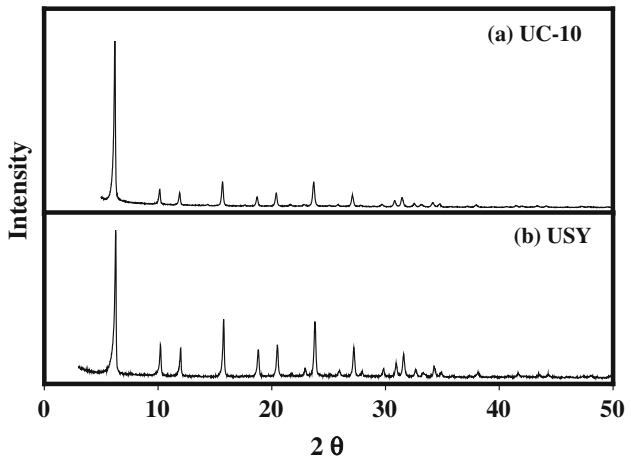

Fig. 3 XRD patterns of the USY and UC-ten adsorbents

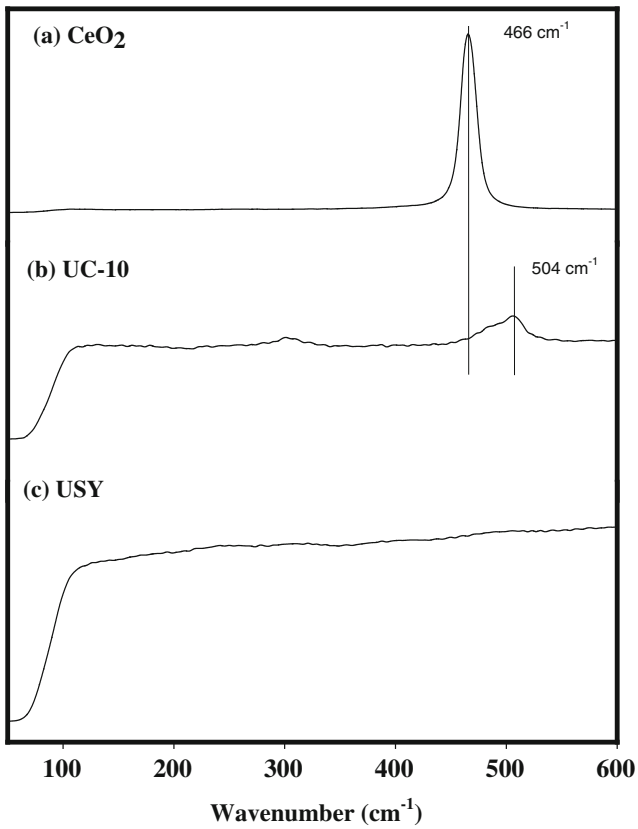

Fig. 4 FT-Raman patterns of the CeO_2, UC-10 and USY adsorbents

For the UC-10 adsorbent, a peak was observed at 504 cm^{-1}, which was assigned to the effect of CeO_2 on USY. According to the work of Garcia et al. (2011), this characteristic peak was related to a higher degree of NH_4^+–Ce^{3+} ion exchange process. In addition, the expected limit of exchange was about 13 wt%, So that the excess cerium in non-exchangeable sites formed small CeOx species, which were responsible for the observed Raman shift (Garcia et al. 2011). In our work, the USY was of Na^+ form, and therefore, the peak of 504 cm^{-1} was related to the degree of Na^+–Ce^{3+} ion exchange. It was found that the Ce form of the UC-10 adsorbent was due to the linking of sites like Ce^{3+}–Na^+ on USY, and the sulfur adsorption performance of the adsorbent was improved by this Ce^{3+}–Na^+ on USY.

We also investigated the effect of different levels of Ce in USY on DMDS and DMS adsorption capacities using the fixed-bed reactor. Figure 5 shows the DMDS and DMS adsorption capacities of various adsorbents according to the amount of Ce. As shown in Fig. 5, the DMDS and DMS adsorption capacities of CeO_2 were only about 2.2 and 2.0 mgS/g sorbent, respectively, which were substantially lower than those of other adsorbents. However, the DMDS and DMS adsorption capacities of USY treated with increasing amounts of Ce increased up to a Ce loading of 10 wt%, and at a loading of 30 % these reduced to 3.2 and 2.5 mgS/g sorbent, respectively. As mentioned previously, in the case of the Ce amount <10 wt%, the degree of the Na^+–Ce^{3+} ion exchange was gradually increased, which also caused an increase of sulfur removing capacity. In the case of Ce amount >10 wt%, The CeO_2 formed from the excess Ce ion source, covered the Na^+–Ce^{3+} ion exchange site, which caused the decrease of sulfur removing capacity (Garcia et al. 2011). Accordingly, UC-10 at a Ce loading of

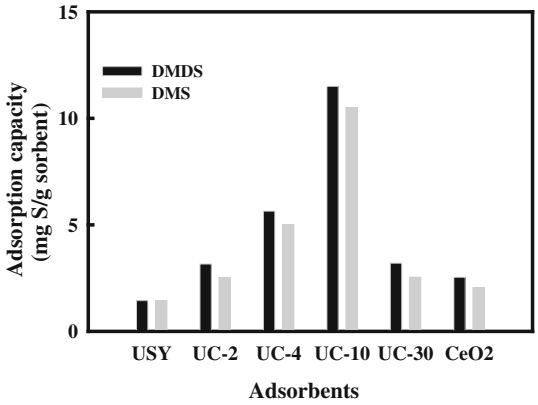

Fig. 5 Sulfur adsorption capacities of various adsorbents for different amounts of Ce

10 wt% was found to have the highest sulfur adsorption capacity of 11.5 mgS/g sorbent.

In previous studies, Watanabe et al. (2003) reported that the sulfur adsorption capacities of adsorbents promoted CeO_2 in TiO_2 and CeO_2-based adsorbents with the addition of promoters Y and La (Watanabe et al. 2004) were about 6–8.5 mgS/g sorbent, which concurred with our findings. However, the organosulfur adsorption capacity of UC-10 adsorbent determined in the present study was higher than any previously reported value for a Ce-based adsorbent.

3.4 Sulfur adsorption by UC-10 adsorbent over multiple cycles

To determine the long-term stability of UC-10 adsorbent, the desulfurization and regeneration processes were repeated for several cycles. Figure 6 shows the DMDS and DMS adsorption capacities of UC-10 adsorbent over several cycles. When both sulfur adsorption and regeneration are considered as one-cycle process, the X-axis was cycle number, and Y-axis was DMDS or DMS adsorption capacities from *n*-hexane over several cycles. As shown in Fig. 6, the DMDS and DMS adsorption capacities of UC-10 adsorbent were about 11–12 mgS/g sorbent over the first cycle. However, DMDS and DMS adsorption capacities during the second cycle were approximately 6 and 5 mgS/g sorbent, respectively, and were maintained at these levels until the fifth cycle. We believed that an undetermined sulfur component was retained by Na^{+}–Ce^{3+} site in the UC-10 adsorbent during cycling.

So far, adsorption properties of sulfur compounds DMDS and DMS in hexane have been determined. We investigated the adsorption capacity of the developed materials for sulfur compounds like DMDS and DMS in real LPG. Figure 7 shows the total adsorption capacity of DMDS and DMS in real LPG on the UC-10 adsorbent at a pressure of 10 bar. Real LPG was supplied by the S-Oil company in Ulsan, and contained 14 and 10 ppm DMDS and DMS, respectively. The LPG feed flow rate was 6 mL/min (liquid phase) at 10 bar. Total adsorption capacity was calculated by summing DMDS and DMS adsorption capacities, and those of UC-10 for DMDS and DMS in real LPG at 10 bar are shown in Fig. 7. As shown in Fig. 7, the total sulfur adsorption capacity of UC-10 adsorbent was about 11.8 mgS/g sorbent during the first cycle, and decreased to about 6 mgS/g sorbent for the second cycles, and was then maintained at relative stability for 20 cycles, which was in line with the DMDS or DMS adsorption capacity results shown in Fig. 6. The DMDS and DMS adsorption capacities of UC-10 adsorbent were not affected by C4 oil components such as, *n*-butane, *n*-butane, and *iso*-butane. It was found that the UC-10 adsorbent was very selective for DMDS and DMS without interference from solvents such as hexane and butane-base. In conclusion, UC-10 adsorbent was found to have excellent organosulfur adsorption capacities, which were substantially retained after the second cycle, and the level of regeneration was higher than that of commercial adsorbents.

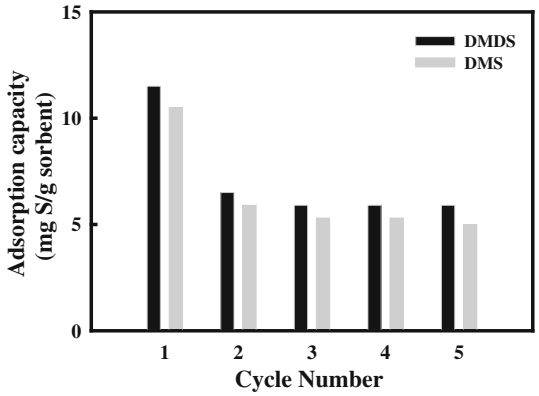

Fig. 6 Sulfur adsorption capacities of UC-10 adsorbent over multiple process cycles

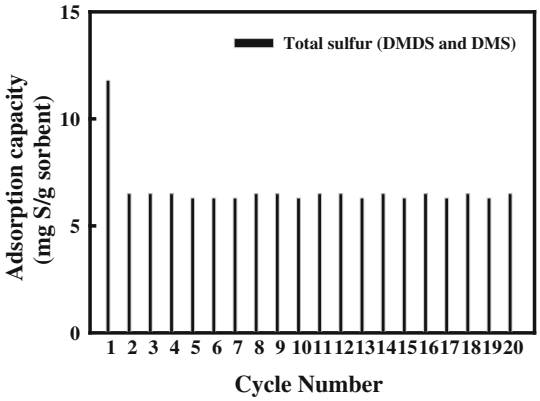

Fig. 7 Long-term stability of UC-10 adsorbent over multiple process cycles for real LPG

4 Conclusions

To remove DMDS and DMS from LPG, we devised an adsorption process based on adsorbents which were with rare earth metals. The various adsorbents produced were tested in a flow liquid reaction system, and the DMDS and DMS adsorption capacities of adsorbents containing Ce, La, and Pr, that is UC-10, UL-10, UP-10 were compared with those of the commercial adsorbents USY and Zeolite Y. In the case of UL-10 and UP-10 adsorbent, DMS adsorption capacities were greater than those of commercial adsorbents, but DMDS adsorption capacities were similar. However, UC-10 adsorbent, that is USY impregnated with Ce, had excellent DMDS and DMS adsorption capacities of 12.5 mgS/g sorbent, which was higher than that of any other adsorbent examined. The form of Ce promoter in UC-10 adsorbent was assigned to the linkage of sites like Ce^{3+}–Na^{+} on USY. The surface area and pore volume of the UC-10 adsorbent were lower than those of the USY adsorbent, but this did not adversely affect its adsorption capacity. Instead, sulfur adsorption capacity appeared to depend on the amount of impregnated Ce. Over multiple process cycles, the LPG sulfur adsorption capacity of UC-10 adsorbent was maintained at 6.0 mg S/g adsorbent from the second to the twentieth cycle, when operated at 10 bars. We believe that the UC-10 adsorbent is highly suitable for the removal of organosulfur compounds from LPG.

Acknowledgments We acknowledge the financial support by grants from Korea CCS R&D center and Priority Research Centers program through the National Research Foundation(NRF) of Korea(Grant no. 2009-0093819), funded by the Ministry of Education, Science and Technology of Korean government.

References

Andersen, K.B., Hansen, M.J., Feilberg, A.: Minimization of artifact formation of dimethyl disulphide during sampling and analysis of methanetiol in air using solid sorbent materials. J. Chromatogr. A **1245**, 24–31 (2012)

Bashkova, S., Bagreev, A., Bandosz, T.J.: Adsorption of methyl mercaptan on activated carbons **36**(12), 2777–2782 (2002)

Basu, B., Satapathy, S., Bhatnagar, A.K.: Merox and related metal phthalocyanine catalyzed oxidation processes. Catal. Rev. Sci. Eng. **35**(4), 51–609 (1993)

Bentley, R., Chasteen, T.G.: Environmental VOSCs-formation and degradation of dimethyl sulfide, methanethiol and related materials. Chemosphere **55**, 291–317 (2004)

Caleron, B., Aracil, I., Fullana, A.: Deodorization of a gas stream containing dimethyl disulfide with zero-valent iron nanoparticles. Chem. Eng. J. **183**, 325–331 (2012)

Chen, H.H., Weng, C.C., Liao, J.D., Whang, L.M., Kang, W.H.: Conversion of emitted dimethyl sulfide into eco-friendly species using low-temperature atmospheric argon micro-plasma system. J. Hazard. Mater. **201–202**, 185–192 (2012)

Chen, T., Jang, M.: Secondary organic aerosol formation from photooxidation of a mixture of dimethyl sulfide and isoprene. Atmos. Environ. **46**, 271–278 (2012)

Cui, H., Turn, S.Q.: Adsorption/desorption of dimethylsulfide on activated carbon modified with iron chloride. Appl. Catal. B **88**, 25–31 (2009)

Demeestere, K., Dewulf, J., Witte, B.D., Langenhove, H.V.: Titanium dioxide mediated heterogeneous photocatalytic degradation of gaseous dimethyl sulfide: parameter study and reaction pathways. **60**, 93–106 (2005)

Devulapelli, V.G., Demessie, E.S.: Catalytic oxidation of dimethyl sulfide with ozone: effects of promoter and physic-chemical properties of metal oxide catalysts. Appl. Catal. A **348**, 86–93 (2008)

Demessie, E.S., Devulapelli, V.G.: Oxidation of methanol and total reduced sulfur compounds with ozone over V_2O_5/TiO_2 catalyst: effect of humidity. Appl. Catal. A **361**, 72–80 (2009)

Eric, D., Guilliaume, D., Annabelle, C., Catherine, C., Abdeltif, A., Diane, T., Yves, A., Pierre, L.C.: Hydrophobic VOC absorption in two-phase partitioning bioreactors; influence of silicone oil volume fraction on absorber diameter. Chem. Eng. Sci. **71**, 146–152 (2012)

Garcia, F.A.C., Araújo, D.R., Silva, J.C.M., Macedo, J.L.de, Ghesti, G.F., Dias, S.C.L., Dias, J.A., Filho, G.N.R.: Effect of cerium loading on structure and morphology of modified Ce-USY zeolites. J. Braz Chem. Soc. **22**(10), 1894–1902 (2011)

Gochi, Y., Ornelas, C., Paraguay, F., Fuentes, S., Alvarez, L., Rico, J.L., Alonso-Nunez, G.: Effect of sulfidation on Mo–W–Ni trimetallic catalysts in the HDS of DBT. Catal. Today **107–108**, 531–536 (2005)

He, J., Zhao, J.B., Lan, Y.X.: Adsorption and photocatalytic oxidation of dimethyl sulfide and ethyl mercaptan over layered $K_{1-2x}Mn_xTiNbO_5$ and $K_{1-2x}Ni_xTiNbO_5$. J. Fuel Chem. Technol. **37**(4), 485–488 (2009)

Hwang, C.L., Tai, N.H.: Removal of dimetylsulfide by adsorption on ion-exchanged zeolites. Appl. Catal. B **93**, 363–367 (2010)

Hwang, C.L., Tai, N.H.: Vapor phase oxidation of dimethyl sulfide with ozone over ion-exchanged zeolites. Appl. Catal. A **393**, 251–256 (2011)

Jarrige, J., Vervisch, P.: Decomposition of gaseous sulfide compounds in air by pulsed corona discharge. Plasma Chem. Plasma Process **27**, 241–255 (2007)

Jo, W.K., Hwang, E.S.: Removal of dimethyl sulfide utilizing activated carbon fiber-supported photocatalyst in continuous-flow system. J. Hazard. Mater. **191**, 234–239 (2011)

Kim, D.J., Yie, J.E.: Role of copper chloride on the surface of activated carbon in adsorption of methylmercaptan. J. Colloid Interface Sci. **283**(2), 311–315 (2005)

Park, J.J., Jung, S.Y., Ryu, C.Y., Park, C.G., Kim, J.N., Kim, J.C.: The removal of sulfur compounds using activated carbon-based sorbents impregnated with alkali or alkaline earth metal. J. Nanoelectron. Optoelectron. **5**, 222–226 (2010)

Park, J.J., Park, C.G., Jung, S.Y., Lee, S.C., Ragupathy, D., Kim, J.C.: Simultaneous removal of sulfur and nitrogen compounds in the C4 gas from fluidized catalytic cracking using modified activated carbons. J. Nanoelectron. Optoelectron. **6**, 306–309 (2011)

Watanabe, S., Ma, X., Song, C.: Selective sulfur removal from liquid hydrocarbons over regenerable CeO_2-TiO_2 adsorbents for fuel cell applications. Am Chem Soc Div Fuel Chem **49**(2), 511–513 (2004)

Watanabe, S., Velu, S., Ma, X., Song, C.: New ceria-based selective adsorbents for removing sulfur from gasoline for fuel cell applications. Am Chem Soc Div Fuel Chem **48**(2), 695–696 (2003)